Dynamic Motion Artifact Removal using Inertial Sensors for Mobile BCI

Byung Hyung Kim, Jinsung Chun, and Sungho Jo, *Member, IEEE*

***Abstract*— EEG signals are vulnerable to several noise and artifacts occurred by muscle activities and body movements. Reducing these artifacts has been a challenge issue to design and develop a reliable mobile EEG system for various real-life applications including home entertainment as well as clinical monitoring, assessment and rehabilitation. In this paper, we describe a method for removing motion artifacts occurred by body movement using inertial sensors. The key contribution of this work is the automatic identification of independent components representing motion artifacts from EEG signals, incurring minimal computation in real-time. The experimental results from the application of the method show that it is able to remove, in real-time, the motion noise of body movement in an real-world environment with improving the quality of EEG signals up to 82% compared with recorded in seated condition.**

I. Introduction

Recently, many studies have focused on researching and developing mobile electroencephalogram (EEG)-based brain-computer interfaces (BCIs), which are able to translate naturally from human behaviors to EEG dynamics for a daily life [1]. The most important requirement in mobile BCIs is to ensure high quality of EEG signals in real-world environments of daily life. However, this requirement has been considered as one of the biggest challenge problems, because EEG signals are vulnerable to various noise and artifacts occurred by muscle activities and body movements. In particular, motion artifacts due to body movements share the same frequency spectra with EEG (up to 50Hz) and have an amplitude that is an order of magnitude larger than the underlying brain-related EEG signals [2]. Although some studies have suggested various methods to obtain high quality of EEG signals against motion artifacts, most of these studies have been limited to highly-controlled laboratory environments such as walking on a treadmill [3]. In this paper, we describe a method for removing motion artifacts occurred by body movements using inertial sensors such as an accelerometer and a gyroscope. Whereas previous studies that used inertial sensors [4], [5] abandoned EEG signals when they are contaminated by motion artifacts detected from inertial sensors, the key contribution of the proposed work is to subtract motion artifacts from the contaminated EEG signals so as to restore them to be comparable to EEG signals obtained in seated condition. The main technical challenge in designing the proposed system was to identify motion artifacts automatically from the contaminated EEG signals. In order to overcome this challenge, we employed two inertial sensors, an accelerometer and a gyroscope, to measure 3-axis acceleration and angular velocity, respectively. Associating them with motion artifacts is ideal because it can measure how much the human body has swayed in real time. For automatic identification of motion artifacts from EEG signals, we first used independent component analysis (ICA) to decompose EEG signals and inertial measurement units (IMUs) measurements into a number of independent components. However, the identification and interpretation of independent components is time-consuming and involves subjective decision making. Therefore, as second step, we developed and an automatic tool designed for separating motion-related independent components from EEG recordings based on the similarities with components from IMU measurements.

The proposed method has been tested on both simulated and real-world data collected from a head-band type EEG device including a Google Nexus 5 mobile phone. The attained accuracy from both datasets is comparable to that obtained in seated condition.

B. Kim, J. Chun, and S. Jo are with the Department of Computer Science, Korea Advance Institute of Science and Technology, Daejeon, Korea (e-mail: {bhyung, trustarpia, shjo}@ kaist.ac.kr).

II. Removing Motion-Related Noise with IMU

Our goal is to restore the quality of contaminated EEG signals, with help of IMUs, to be comparable to the signals recorded in seated condition. Fig. 1 shows the overview of our work. We implemented a two-steps approach to removing motion artifacts in EEG signals. First, EEG signals and IMU measurements are decomposed into a number of components. The components decomposed from EEG signals represent brain-related signals and motion-related signals. On the other hand, the components decomposed from IMU measurements mostly represent motion-related signals. Next step, we find

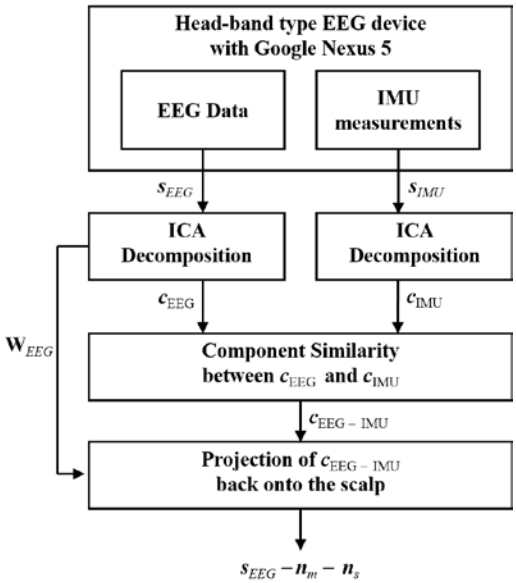

Fig. 1. The overview for removing motion artifacts from EEG signals

similar EEG components to that of most other IMU components. Based on the similarities between two components, the matched components are used to remove motion artifacts from EEG signals. Details are described in the following subsections.

A. Decomposing signals into components

Human body motion measurements are fused with measurements from a 3-axis gyroscope and accelerometer, which provide the rotational velocity $\boldsymbol{\omega}_m$ and acceleration $\boldsymbol{\alpha}_m$, respectively:

$$\boldsymbol{\omega}_m = \boldsymbol{\omega} + \boldsymbol{b}_g + \boldsymbol{n}_r \quad (1)$$

$$\boldsymbol{\alpha}_m = \boldsymbol{\alpha} + \boldsymbol{b}_a + \boldsymbol{n}_a \quad (2)$$

where $\boldsymbol{\omega}$ and $\boldsymbol{\alpha}$ are the IMU's rotational velocity vector and acceleration respectively, $\boldsymbol{b}_g$ and $\boldsymbol{b}_a$ are the gyroscope and accelerometer biases, respectively, and finally $\boldsymbol{n}_r$ and $\boldsymbol{n}_a$ are zero-mean white Gaussian noise vector affecting the measurements. These two measurements (1) and (2) are concatenated into:

$$\boldsymbol{s}_{IMU} = [\, \boldsymbol{s}^{(x)}_{IMU}, \boldsymbol{s}^{(y)}_{IMU}, \boldsymbol{s}^{(z)}_{IMU} \,]^{\mathrm{T}} \quad (3)$$

where $\boldsymbol{s}^{(i)}_{IMU} = [\boldsymbol{\omega}_m, \boldsymbol{\alpha}_m]$, for $i = x, y$ and z axis. Human brain dynamics are recorded into EEG signals as the sum of a true underlying EEG signals and various artifacts:

$$\boldsymbol{s}_{EEG} = \boldsymbol{s} + \boldsymbol{n}_m + \boldsymbol{n}_s \quad (4)$$

where $\boldsymbol{s}$ is a true EEG underlying EEG signal vector, $\boldsymbol{n}_m$ is a motion artifact vector, and $\boldsymbol{n}_s$ is a zero-mean white Gaussian noise vector affecting the measurements

Each of the two measurements (3) and (4) are decomposed into n and m independent components $\boldsymbol{c}_{\mathrm{IMU}}$ and $\boldsymbol{c}_{\mathrm{EEG}}$, respectively. The decomposition is carried out by ICA, which is a computational method for separating sources into additive subcomponents supposing the mutual statistical independence of the non-Gaussian source signal. The objective of the ICA algorithm is to find a separating matrix $\mathbf{W}$:

$$\boldsymbol{c} = \mathbf{W}\boldsymbol{s} \quad (5)$$

where $\boldsymbol{c}$ is independent components and $\boldsymbol{s}$ is measured sources. Therefore, in our study, each of (3) and (4) are inputted as $\boldsymbol{s}$ and $\boldsymbol{c}_{\mathrm{IMU}}$ and $\boldsymbol{c}_{\mathrm{EEG}}$ are yielded as outputs of (5), respectively.

The next step is to find the most similar n components between $\boldsymbol{c}_{\mathrm{IMU}}$ and $\boldsymbol{c}_{\mathrm{EEG}}$ and get rid of them from $\boldsymbol{c}_{\mathrm{EEG}}$ so that motion artifacts are removed from the contaminated EEG

B. Measuring similarity between two components and cleaning EEG signals

Similarities between two $\boldsymbol{c}_{\mathrm{IMU}}$ and $\boldsymbol{c}_{\mathrm{EEG}}$ are computed by cross-correlation. The computation yields higher peaks when two components are more correlated. Therefore, we chose the highest peaked component from $\boldsymbol{c}_{\mathrm{EEG}}$ measuring similarities with each of all components of $\boldsymbol{c}_{\mathrm{IMU}}$. The chosen n number of components in $\boldsymbol{c}_{\mathrm{EEG}}$ are excluded when the true EEG signal $\boldsymbol{s}$ is obtained by projecting the sum of selected unrelated motion artifactual ICA components back on the scalp.

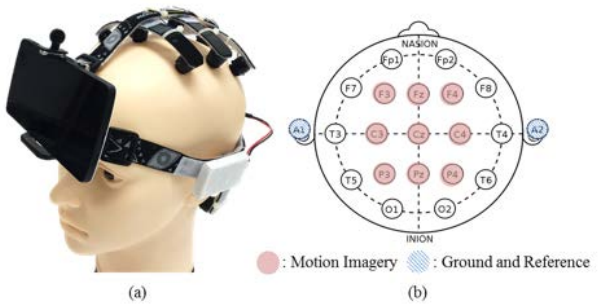

Fig. 2. (a) Head-band type EEG device with Google Nexus 5. (b) The location of 9 electrodes and 2 reference electrodes

C. Algorithm and implementation details

The entire process for removing motion artifacts from EEG signals is described in Fig. 1. The process assumed that EEG signals and IMU measurements can be measured at the same time. However, in practice, the sensor measurements are not sampled at the same time. Furthermore, in fact, the gyroscope and accelerometer in consumer-grade devices are usually separate units, so these two sensors' data arrive at different time instants. For these practical reasons, we implement the interpolation of the inertial measurements so as to be available to receive (1) the gyroscope and accelerometer data simultaneously, and (2) the two sensors' data at the time EEG signal begins.

III. Experiments and Results

A. Experimental Setup

The experiments were conducted using the head-band type EEG device as shown in Fig. 2. A mobile phone (Google Nexus 5) that is equipped with a 3-axis gyroscope and accelerometer is attached to the band type device. The device provides gyroscope at 204Hz and accelerometer measurements at 207Hz. Both measurements were resampled to 200Hz as described in Section II.C. On the other hand, brain signals were recorded at 128Hz. 9 electrodes are located at F3, Fz, F4, C3, Cz, C4, P3, Pz, and P4 of the International 10-20 System for EEG measurements, and 2 reference electrodes were positioned at the left and right earlobe. EEG signals were filtered between 1 and 65Hz to remove all frequencies outside the range.

5 right-handed volunteers (all males, 24~34 years old) participated in the experiments. In order to train their motion imagery, the subjects sat comfortably in armchair hearing audio feedbacks. The duration of each trial was 10 seconds. The first 4 seconds were given for the "relax" state. During the next 2 seconds, a "right" or "left" cue was announced, so that the subjects were asked to imagine the movement during the last 4 seconds.

As EEG features of motor imagery for training and testing, we used the phase locking values (PLV), which is a measurement of the level of phase coupling that occurs between two signals occupying the same narrow frequency range [12]. 5 pairs {(C3, Cz), (C4, Cz), (C3, C4), (C3, Fz), and (C4, Fz)} were selected to classify three classes (left, right,

TABLE I. RESULTS OF PLV VALUES SYNTHETIC SIMULATION

Body Movement	PLV Values			Recovery (%)
	w/o our system		w/ our system	
	True Signal (s)	Contaminated (s_{EEG})	Recovered ($s_{EEG} - n_m - n_s$)	
Head Shaking	0.732±0.006	0.996±0.001	0.556±0.074	82.4±7.5
Head Nodding	0.733±0.003	0.996±0.001	0.606±0.235	77.7±14.3
Free Walking	0.732±0.003	0.996±0.001	0.468±0.149	73.6±14.9

and neutral). For classifying the three classes, we used support vector machines (SVMs) with a linear kernel under one-versus-the rest classification scheme which means the one class is compared to all remaining classes. 10-fold cross-validation was also used to avoid overfitting of the data. The test results in seated condition were reported in the Section III. C. The support vectors and their margin were used to test real-world experiments described in Section III.C

B. Synthetic EEG data simulation

To examine the efficacy of our system to remove motion artifacts occurred by various body movements, we generated synthetic EEG data satisfying (4). $\boldsymbol{n}_m$ and $\boldsymbol{n}_s$ were collected from three types of EEG signals contaminated by actual body movements; head nodding, head shaking, and free walking. The values of $\boldsymbol{n}_m$ and $\boldsymbol{n}_s$ were averaged from 5 subjects who were asked to relax themselves while moving. At the same time, IMU measurements were collected from Google Nexus 5. $\boldsymbol{s}$ was generated from the normal distribution with zero mean and unit variance and then it was multiplied by the standard deviation of $\boldsymbol{n}_m$ and $\boldsymbol{n}_s$ in order to simulate real attributes of EEG artifacts. The $\boldsymbol{s}$ consists of 2 channels and 1280 samples.

We carried out 10 trials, and in each trial we computed the PLV values to evaluate the performance of the proposed system. As shown in Table 1, the motion artifacts increased significantly the PLV values to 1, which means the relationship between two channels was completely lost. Note that the closer the PLV is to 1, the more consistent the phase difference between the paired signals. However, the results with our proposed system show that the PLV values are recovered successfully to be comparable to the one from the true EEG signal $\boldsymbol{s}$. From the three types of body movements, the recovery percentage is up to 82.4%. Fig. 3 also illustrates the efficacy of our proposed system to remove the motion artifacts. The top row in the figure shows the synthetic $\boldsymbol{s}$, the middle shows $\boldsymbol{n}_m$ and $\boldsymbol{n}_s$ from free walking, and the bottom row shows the cleaned $\boldsymbol{s}$ by our system.

C. Real-World Experiments

To test the performance of our proposed algorithm in real-world environment, we designed real life scenarios where people can interact with multiple objects naturally in their living room. In particular, in our scenarios, subjects were asked to control TV volume up or down through imaging left or right hand movements, respectively. Before starting the experiment, EEG signals from each hand

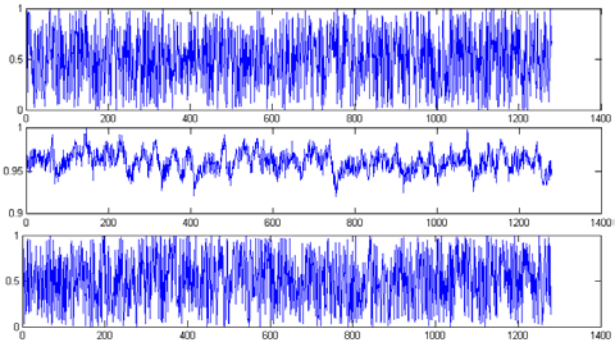

Fig. 3. EEG signals used for synthetic data simulation. (Top) Synthetic EEG data generated from the normal distribution. (Middle) Noise EEG signal obtained from free walking. (Bottom) Cleaned EEG signal by removing some selected IC by ICA. All amplitude of signals are normalized between 0 and 1 for visualization.

movement were recorded in seated condition and they were used for training. The experiments started with 10s for relaxing where the subject was sitting at the table. Until the participant finished his/her task, he/she was requested to imagine right/left movement randomly. Fig. 4 shows the top view of our living room scenarios. Subjects are asked to interact with four items from audio commands as follows:

- Reading the book. The participants were asked to follow the audio command "Please read the book in front of you imaging left/right hand movements in order to control volume up/down during 15s period." The purpose of this experiment is to test the performance of our system against the existence of slow head movements.
- Moving the cup on the table. The testing started when the participants moved the cup counter-clockwise on the table. The task of this experiment consists of moving the cup to four areas A, B, C, and D twice. The purpose of this experiment is to test the performance of our system against the existence of hand and body movements.
- Operating the coffee machine. The testing started when the participant pushed one button on the coffee machine. The task of this experiment consists of pushing four buttons on the machine, returning to the starting point (the table) slowly holding the cup with one hand in time sequence. The purpose of this experiment is to test the performance of our system

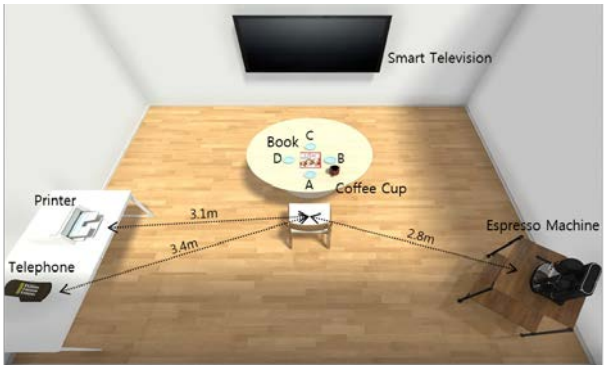

Fig. 4. Real-world Scenarios Environment

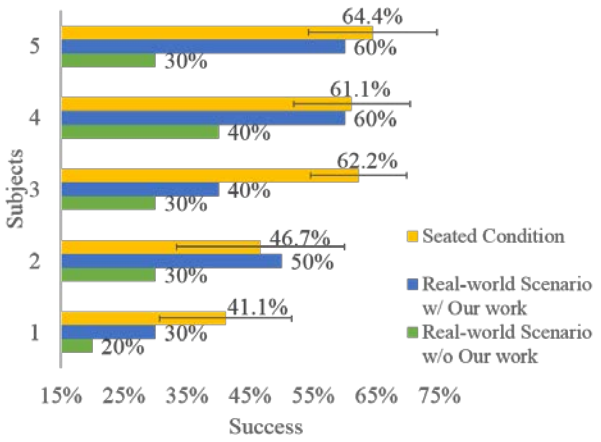

Fig. 5. Results of Real-world Experiments

against the existence of hand and slow body movements.

- Printing a paper. The testing started when the participant pushed one button on the printer. The task of this experiment consists of loading a paper into the printer, grabbing a paper on the printer, and returning to the starting point rapidly holding the paper with two hands. The purpose of this experiment is to test the performance of our system against the existence of hand and quick body movements.
- Receiving a phone call while watching the TV. The testing started when the participant received a phone call on the desk. The task of this experiment consists of holding a phone, turning his/her head to watch the TV during 5s, and returning to the starting point. The purpose of this experiment is to test the performance of our system against the existence of hand, quick head and body movements.

In our experiments, all subjects took at least 17s to complete each of the 5 scenarios. Therefore, we randomly chose 14s EEG and IMU data segments. Each of two segments was split into four 4s-sized windows. Given four windows, the windows which contain left/right imagination are used for classification described in the section III.A. The success of a task is determined if two consecutive classification results are identical to the one from the audio command. Each participant was ask to repeat each scenario twice. So, 10 trials were used to calculate success percentages. Fig. 5 shows the success percentages of the real-world experiments. Whereas all participants rarely have succeed without motion artifacts, the success rate increased up to averaged 60% with help of our proposed system. 60% may not satisfy all the requirements for real-world applications. However, we would address achieving high accuracy for multi-class problems has been the most difficult challenge problem in current BCI areas [6], [7]. Alternatively, our proposed method recovered the contaminated EEG up to averaged 87.1%. Therefore, this shows the proposed system recovered the contaminated EEG signals robustly with respect to accuracy comparable to the result obtained in seated condition. During the real world experiments, artifacts occurred by any eye movements were not considered in this study. This may decrease the effectiveness of recovering the true EEG signals. Although some studies have suggested automated methods to detect and remove eye artifacts using ICA, we have not treated the artifacts as a part of motion artifacts in order to emphasize the performance of our system for removing motion artifacts occurred by body movements.

IV. Conclusion

In this paper, we have presented an algorithm for removing motion artifacts from EEG signals using inertial sensors. To model the effect of inertial sensors the proposed method decomposes both EEG and IMU data using ICA and identify motion artifacts based on similarity between two components. Our experimental testing has shown that the method is capable of recovering the contaminated EEG comparable to the one obtained in seated condition in real time: in our tests, the algorithm removed the motion artifacts occurred by various body movements with approximately 78% of recovery performance. These results indicate that the proposed approach is suitable for real-time mobile BCIs of miniature devices.

Acknowledgment

This work was supported by Basic Science Research Program through the National Research Foundation of Korea funded by the Ministry of Education (2013R1A1A2009378).

References

[1] K. Mcdowell, C.-T. Lin, K. S. Oie, T.-P. Jung, S. Gordon, K. W. Whitaker, S.-Y. Li, S.-W. Lu, and W. D. Hairston, “Real-world neuroimaging technologies,” *IEEE Access*, Vol. 1, pp. 131–149, May, 2013.

[2] J. T. Gwin, K. Gramann, S. Makeig, and D. P. Ferris, “Removal of movement artifact from high-density EEG recorded during walking and running,” *Journal of neurophysiology*, Vol. 103, No. 6, pp. 3526–3534, 2010.

[3] Y. P. Lin, Y. Wang, C. S. Wei, and T. P. Jung, “Assessing the quality of steady-state visual-evoked potentials for moving humans using a mobile electroencephalogram headset,” *Frontiers in human neuroscience*, vol. 8, 2014.

[4] S. O’Regan, S. Faul, and W. Marnane, “Automatic Detection of EEG Artefacts Arising from Head Movements Using EEG and Gyroscope Signals,” *Medical Engineering & Physics*, vol. 35, no. 7, pp. 857–874, 2013.

[5] K. T. Sweeney, D. J. Leamy, T. E. Ward, and S. McLoone, “Intelligent Artifact Classification for Ambulatory Physiological Signals,” in *EMBC*, pp. 6349–6352, 2010.

[6] B. Kim, M. Kim, and S. Jo, "Quadcopter flight control using a low-cost hybrid interface with EEG-based classification and eye tracking," *Computers in Biology and Medicine*, vol.51, pp. 82-92, 2014.

[7] B. Choi and S. Jo, "A low-cost EEG system-based hybrid brain-computer interface for humanoid robot navigation and recognition," *PLoS ONE* 8(9):e74583, 2013.